Fast STED microscopy with continuous wave fiber lasers

Gael Moneron,[1] Rebecca Medda,[1] Birka Hein,[1] Arnold Giske,[2] Volker Westphal,[1] and Stefan W. Hell[1]*

[1]Department of NanoBiophotonics, Max Planck Institute for Biophysical Chemistry, Am Fassberg 11, 37077 Göttingen, Germany
[2]Advanced Technology Group, Leica Microsystems CMS GmbH, Am Friedensplatz 3, 68165 Mannheim, Germany
*shell@gwdg.de

Abstract: We report on fast beam-scanning stimulated-emission-depletion (STED) microscopy in the visible range using for resolution enhancement compact, low cost and turn-key continuous wave (CW) fiber lasers emitting at 592 nm. Spatial resolutions of 35 to 65 nm in the focal plane are shown for various samples including fluorescent nanoparticles, immuno-stained cells with a non-exhaustive selection of 5 commonly used organic fluorescent markers, and living cells expressing the yellow fluorescent protein Citrine. The potential of the straightforward combination of CW-STED and fast beam scanning is illustrated in a movie of the endoplasmic reticulum (ER) of a living cell, composed of 100 frames (6 µm × 12 µm), each of them acquired in a time shorter than 0.2 s.

OCIS codes: (180.1790) Confocal microscopy; (180.2520) Fluorescence microscopy; (180.5810) Scanning microscopy; (110.0180) Microscopy.

References and links

1. S. W. Hell, and J. Wichmann, "Breaking the diffraction resolution limit by stimulated emission: stimulated-emission-depletion fluorescence microscopy," Opt. Lett. **19**(11), 780–782 (1994).
2. S. W. Hell, "Microscopy and its focal switch," Nat. Methods **6**(1), 24–32 (2009).
3. T. A. Klar, and S. W. Hell, "Subdiffraction resolution in far-field fluorescence microscopy," Opt. Lett. **24**(14), 954–956 (1999).
4. V. Westphal, and S. W. Hell, "Nanoscale resolution in the focal plane of an optical microscope," Phys. Rev. Lett. **94**(14), 143903 (2005).
5. G. Donnert, J. Keller, R. Medda, M. A. Andrei, S. O. Rizzoli, R. Lührmann, R. Jahn, C. Eggeling, and S. W. Hell, "Macromolecular-scale resolution in biological fluorescence microscopy," Proc. Natl. Acad. Sci. U.S.A. **103**(31), 11440–11445 (2006).
6. E. Rittweger, K. Y. Han, S. E. Irvine, C. Eggeling, and S. W. Hell, "STED microscopy reveals crystal colour centres with nanometric resolution," Nat. Photonics **3**(3), 144–147 (2009).
7. K. I. Willig, S. O. Rizzoli, V. Westphal, R. Jahn, and S. W. Hell, "STED microscopy reveals that synaptotagmin remains clustered after synaptic vesicle exocytosis," Nature **440**(7086), 935–939 (2006).
8. R. R. Kellner, C. J. Baier, K. I. Willig, S. W. Hell, and F. J. Barrantes, "Nanoscale organization of nicotinic acetylcholine receptors revealed by stimulated emission depletion microscopy," Neuroscience **144**(1), 135–143 (2007).
9. A. C. Meyer, T. Frank, D. Khimich, G. Hoch, D. Riedel, N. M. Chapochnikov, Y. M. Yarin, B. Harke, S. W. Hell, A. Egner, and T. Moser, "Tuning of synapse number, structure and function in the cochlea," Nat. Neurosci. **12**(4), 444–453 (2009).
10. C. Eggeling, C. Ringemann, R. Medda, G. Schwarzmann, K. Sandhoff, S. Polyakova, V. N. Belov, B. Hein, C. von Middendorff, A. Schönle, and S. W. Hell, "Direct observation of the nanoscale dynamics of membrane lipids in a living cell," Nature **457**(7233), 1159–1162 (2009).
11. V. Westphal, S. O. Rizzoli, M. A. Lauterbach, D. Kamin, R. Jahn, and S. W. Hell, "Video-rate far-field optical nanoscopy dissects synaptic vesicle movement," Science **320**(5873), 246–249 (2008).
12. U. V. Nägerl, K. I. Willig, B. Hein, S. W. Hell, and T. Bonhoeffer, "Live-cell imaging of dendritic spines by STED microscopy," Proc. Natl. Acad. Sci. U.S.A. **105**(48), 18982–18987 (2008).
13. B. Harke, J. Keller, C. K. Ullal, V. Westphal, A. Schönle, and S. W. Hell, "Resolution scaling in STED microscopy," Opt. Express **16**(6), 4154–4162 (2008).
14. K. I. Willig, B. Harke, R. Medda, and S. W. Hell, "STED microscopy with continuous wave beams," Nat. Methods **4**(11), 915–918 (2007).
15. A. Schönle, Imspector Image Acquisition & Analysis Software, v0.1, (2006): http://www.imspector.de

16. O. Griesbeck, G. S. Baird, R. E. Campbell, D. A. Zacharias, and R. Y. Tsien, "Reducing the environmental sensitivity of yellow fluorescent protein," J. Biomed. Chem. **276**(31), 29188–29194 (2001).
17. B. Hein, K. I. Willig, and S. W. Hell, "Stimulated emission depletion (STED) nanoscopy of a fluorescent protein-labeled organelle inside a living cell," Proc. Natl. Acad. Sci. U.S.A. **105**(38), 14271–14276 (2008).
18. D. Wildanger, E. Rittweger, L. Kastrup, and S. W. Hell, "STED microscopy with a supercontinuum laser source," Opt. Express **16**(13), 9614–9621 (2008).
19. D. Wildanger, J. Bückers, V. Westphal, S. W. Hell, and L. Kastrup, "A STED microscope aligned by design," Opt. Express **17**(18), 16100–16110 (2009).
20. G. Donnert, C. Eggeling, and S. W. Hell, "Major signal increase in fluorescence microscopy through dark-state relaxation," Nat. Methods **4**(1), 81–86 (2007).
21. G. Donnert, C. Eggeling, and S. W. Hell, "Triplet-relaxation microscopy with bunched pulsed excitation," Photochem. Photobiol. Sci. **8**(4), 481–485 (2009).
22. List of fluorescent dyes used in STED microscopy: *http://www.mpibpc.mpg.de/abteilungen/200/STED_Dyes.htm*

1. Introduction

The introduction of stimulated-emission-depletion (STED) microscopy [1] for overcoming the resolution diffraction-barrier in far-field fluorescence microscopy and of numerous complementary methods [2] has opened new opportunities in biology as well as in other fields of research. The growing interest for these so-called far-field optical nanoscopy techniques is obviously accompanied by the need for fast acquisition speed in order to investigate nano-scale dynamics or to freeze motions in living samples without loosing the advantage of the high-resolution. STED microscopy has proven to be a powerful approach for sub-diffraction imaging [3–6], applied in the exploration of various biological questions [7–10], and has shown to be suited for marrying high-resolution and live imaging [11,12].

The sub-diffraction resolution of STED microscopy is reached by scanning a sub-diffraction fluorescence-probing volume in the sample obtained by prohibiting signaling by spontaneous emission of the molecules located in the periphery of the diffraction-limited excitation area via stimulated emission. For that purpose a STED beam, red-shifted with respect to the fluorescence maximum and out of the spectral detection window, is injected into the microscope such that it typically produces a doughnut-shaped focal pattern featuring a zero-intensity point overlapping with the excitation maximum in the focal plane. Stimulated emission essentially deprives the fluorophores of their ability to fluoresce (i.e. turns them off) and, in combination with this light distribution, a theoretically unlimited resolution is obtained that is given by Eq. (1) [4,13]:

$$d_{STED} \approx \lambda \big/ \left(2NA\sqrt{1+I/I_S}\right), \tag{1}$$

with the wavelength of light λ, the numerical aperture of the objective lens *NA*, the intensity at the maximum of the STED doughnut *I*, and a saturation intensity I_S characteristic of the dye.

So far, only complex and relatively expensive laser systems have been used in fast beam-scanning configurations for STED microscopy, although the elegance of the STED implementation with CW lasers [14] and a fast beam-scanner can be advantageously combined as discussed below. We report in the present article on such a combination using visible fiber-lasers for resolution enhancement, and we demonstrate its large potential with 5 different commonly used organic fluorescent markers, as well as with the yellow fluorescent protein (YFP) Citrine.

2. Setup

The setup sketched in Fig. 1 was a custom fast-beam scanning microscope using a 15 kHz resonant scanning mirror (SC-30, EOPC, USA) for the fast axis and a piezo-stage (PXY 36 CAP, Piezosystem Jena, Germany) for the slow axis. The excitation light at 488 nm was provided by an Argon laser (Innova 70C, Coherent, USA) and the STED light by two continuous wave (CW) fiber-lasers emitting at 592 nm (VFL-P-1000 592, MPB Communications, Canada) and providing 1W each.
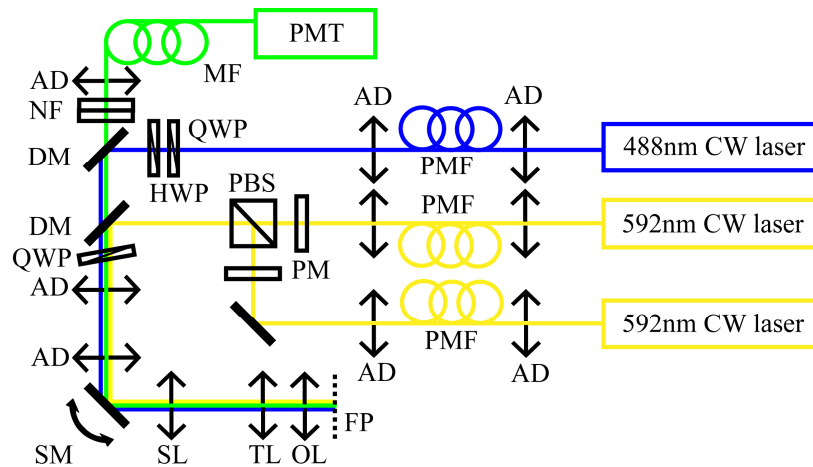
Fig. 1. Experimental setup. The 3 laser beams are injected into single-mode polarization-maintaining fibers (PMF) with achromatic doublets (AD). After collimation, the two STED beams pass through phase masks (PM) and are combined with a polarization beam splitter (PBS). The collinearly aligned beams are then reflected by a dichroic mirror (DM) and circularly polarized by a quarter-waveplate (QWP). They are de-magnified by 2 achromatic doublets, deflected by the scanning mirror (SM) and directed toward the objective lens (OL) by a scan lens (SL) and a tube lens (TL). Before being injected into the microscope, the excitation beam is polarized with a quarter-waveplate and a half-waveplate (HWP) such that its polarization in the back aperture of the objective lens is circular. The fluorescence light passes through notch filters (NF), is injected in a multimode fiber (MF), and finally detected by a photomultiplier (PMT). FP denotes the focal plane.

Before their injection into the microscope, excitation and STED beams were spatially filtered with single-mode polarization-maintaining fibers (PM460HP, Thorlabs; PMC-630-4.6-NA011-3-APC-200-P with a cutoff at 570 nm, Schäfter + Kirchhoff, Germany). The two STED beams passed through two polymer masks imprinting 0 to 2π helical phase-ramps (VPP-A1, RPC Photonics, USA) in order to obtain doughnut-like diffraction patterns at the focus. The two orthogonally linearly polarized STED beams were combined with a polarizing beam splitter before being collinearly aligned with the excitation beam using dichroic mirrors (Z500RDC and Z590SPRDC, AHF Analysentechnik, Germany). The beams were de-magnified by two achromatic doublets in a 4f-configuration (300 mm and 80 mm ARB2 VIS, Linos, Germany), deflected by the resonant scanning mirror, and directed toward the objective lens (HCX PL APO 100 × /1.40–0.7 Oil, Leica Microsystems, Germany) by the same set of scan and tube lenses as the one used in a commercial scanning microscope (Leica TCS SP2, Leica Microsystems, Germany). A symmetrical STED light distribution with a zero-intensity point of less than 1% on the optical axis was obtained in the focal plane by imposing circular polarizations to both STED beams in the back-aperture of the objective lens using a carefully oriented and tilted quarter-waveplate after the dichroic mirror. An ideal isotropic excitation, given by a circular polarization of the excitation beam in the focal plane, was obtained using a half-waveplate and a quarter-waveplate placed before the dichroic mirrors in order to pre-compensate for the alterations of the polarization-states induced mainly by the dichroic mirrors and the other quarter-waveplate adjusted for the STED beams. The fluorescence light, was collected by the same objective lens, de-scanned, passed through the dichroic mirrors as well as through two notch filters (StopLine 488 and StopLine 594, Semrock, USA) before being injected into a multimode fiber (M31L01, Thorlabs) connected to the detector. This multimode fiber played the role of a confocal pinhole with a diameter of the back-projected Airy-disk at 520 nm. Confocal detection is not required for resolution enhancement in a STED microscope, but it helps to improve the signal-to-background ratio of the image by getting rid of the out-of-focus fluorescence. In order to enable high count-rates required for fast acquisition speeds, a photomultiplier with a large dynamic range and a quantum efficiency of

~35% at 520 nm (H7422PA-40, Hamamatsu, Japan) was used for detection. Photon counting and data pre-processing were accomplished with a custom field programmable gate array (FPGA) board [11]. All acquisition operations were automated and managed by the software Imspector [15]. Special care was exerted to optically conjugate the position of the scanning mirror with the back-aperture of the objective lens such that the images of the two phase-masks in that plane were fixed while scanning.

3. Results

For testing the performance of the setup we first recorded confocal and STED images of 20 nm yellow-green fluorescent particles (Yellow-green FluoSpheres, Molecular Probes). The particles were mounted on a microscope cover glass with poly-L-lysine as the linker and 2,2'thiodiethanol (TDE) as embedding medium. The absorption and fluorescence emission maxima of these particles were 505 nm and 515 nm, respectively. Typical images obtained with the described setup are presented in Fig. 2.
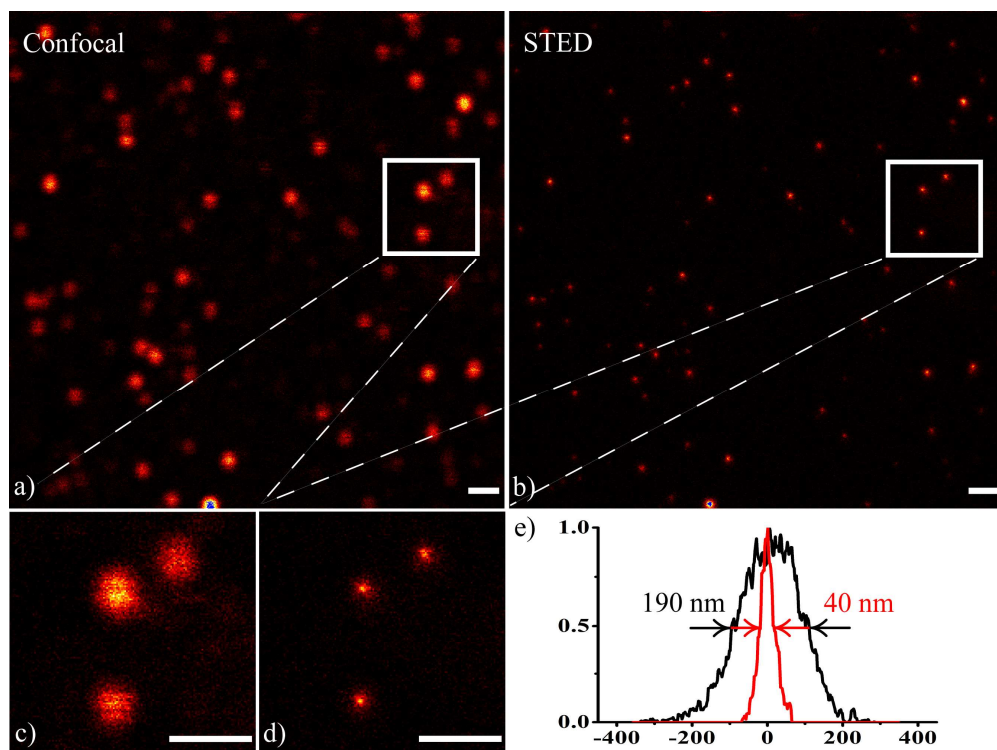

Fig. 2. Comparison of confocal and STED images of 20 nm Yellow-green fluorescent particles mounted on a cover glass. (a) and (b) are, respectively, the raw pictures of obtained in confocal and STED modes. (c) and (d) show enlargements of the areas marked with white squares in (a) and (b), respectively. Scale bars correspond to 500 nm. Normalized intensity profiles of the averaged images over more than 10 single bead images taken from the confocal (a) and from the STED (b) pictures, are plotted in (e) in black and red, respectively.

The CW optical power levels in the back aperture of the objective lens were ~25 µW at 488 nm for excitation and ~600 mW at 592 nm for STED. The central pixel dwell-time was 2.85 µs and the pixel size 10 nm. The resolution enhancement achieved by the only presence of the STED beam is clearly visible in the side-by-side comparison of enlarged raw-images of single particles. A quantitative estimation of the resolution in the STED mode was performed based on the measurement of the full-width-at-half-maximum (FWHM) of the intensity profile of the averaged image over more than 10 different single particle images. The FWHM of the averaged STED profile was in that case 40 nm. Considering the 20 nm particles size

and assuming Gaussian models for the effective point spread function (PSF), the object, and the image intensity profile, the optical resolution was determined to be between 35 and 40 nm. The same statistical analysis was applied to the confocal picture and gave the expected diffraction-limited value of ~190 nm, meaning a 4.8 to 5.4-fold improvement in resolution with STED in the focal plane, or a 9 to 29-fold area reduction over already excellent confocal results.

In order to demonstrate the high potential of 592 nm as a CW-STED wavelength of choice for biological investigation in the visible, we present in Fig. 3 a side-by-side comparison of confocal and STED pictures of vimentin fibers in PtK2 cells labeled with a primary antibody (anti-vimentin mouse IgG [V9], Sigma) and stained with 5 different commonly used markers attached to a secondary antibody (sheep anti-mouse IgG, Dianova). The samples were embedded in Mowiol. The selection of the 5 widely used fluorescent markers shown in Fig. 3 is listed in Table 1. For these results we typically used between 8 and 35 µW for excitation at 488 nm, and ~600 mW for STED at 592nm, in the back aperture of objective lens, in the STED mode. The pixel dwell-times were between 2 and 5 µs for all the pictures and the pixel size 15 nm. Intensity line profiles of the narrowest filaments in all the STED pictures show FWHM of ~70 nm. Since the size of a single vimentin fiber is assumed to be ~10 nm and the length of each primary and secondary antibodies sandwich is ~20 nm, the real size of the narrowest fluorescent structure is assumed to be ~50 nm, meaning that the optical resolution in those conditions was then better than 60 nm.

Table 1. Fluorescent markers used for CW-STED microscopy at 592 nm

Dye	Product name	Company	Absorption maximum	Emission maximum
Oregon green 488	Oregon Green carboxylic acid SE	Invitrogen	498 nm	526 nm
Chromeo 488	Chromeo 488 NHS-Ester	Actif Motif Chromeon	488 nm	517 nm
Alexa 488	Alexa Fluor 488 carboxylic acid SE	Invitrogen	500 nm	520 nm
DY-495	DY-495 NHS-ester	Dyomics	493 nm	521 nm
FITC	Fluorescein-5-isothiocyanate	Invitrogen	496 nm	518 nm

In addition to the large spectrum of applications that could advantageously benefit from the sub-diffraction resolution of CW-STED at 592nm with the non-exhaustive selection of organic dyes listed above, we illustrate next the suitability of the setup for ultra-fast high-resolution live-cell imaging with the yellow fluorescent protein Citrine [16]. So far, Citrine turned out to be the best fluorescent protein tested for STED in the visible range [17]. The absorption and fluorescence emission maxima of Citrine are 516 nm and 529 nm, respectively. In Fig. 4, we show pictures taken from a time-lapse movie of the endoplasmic reticulum (ER) of a living PtK2 cell expressing Citrine.
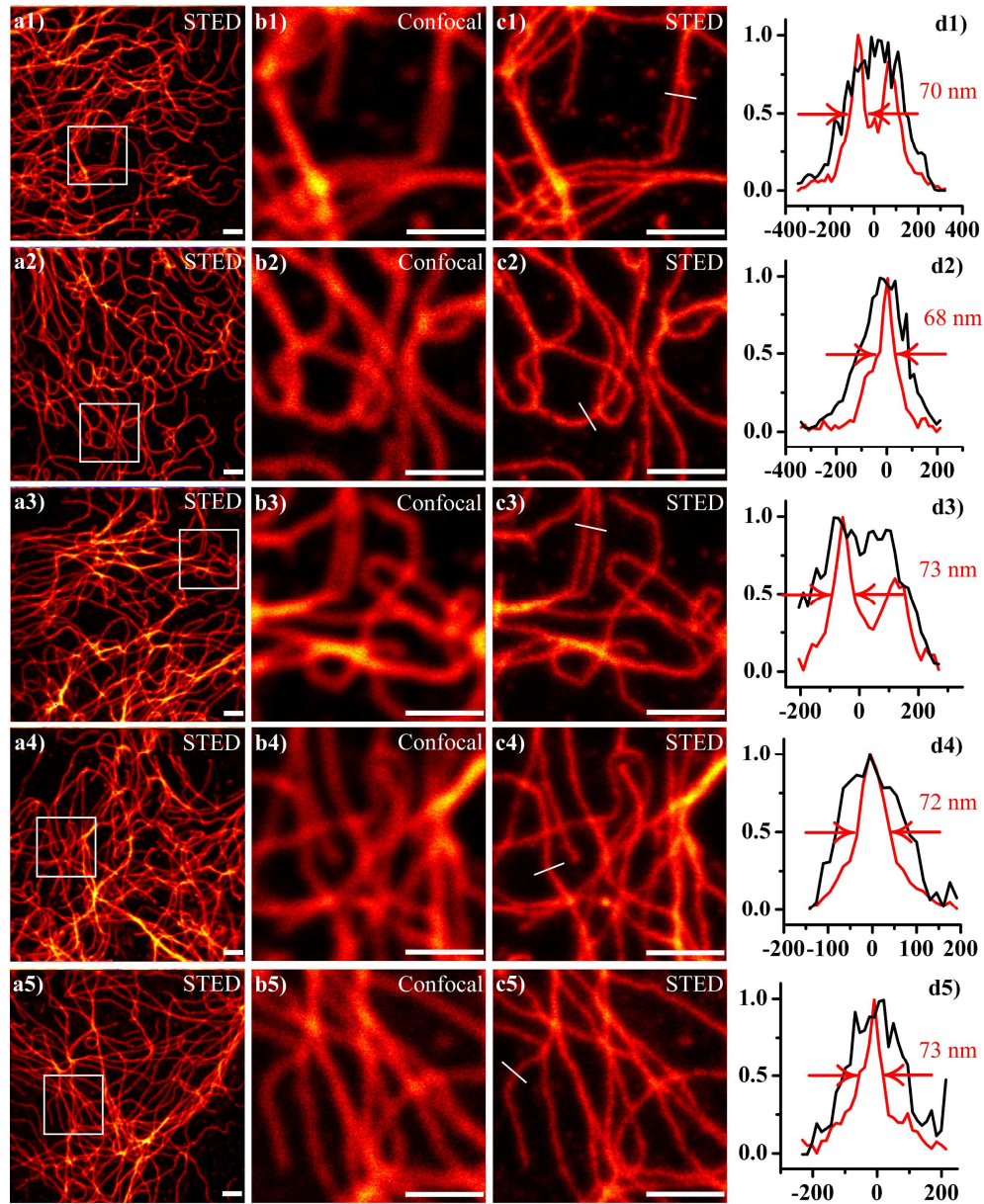
Fig. 3. Demonstration of similar STED resolution enhancements obtained with the same laser configuration for five commonly used organic fluorescent markers. The five dyes were tested on vimentin filaments in PtK2 cells labeled with primary and secondary antibodies. ai) pictures, with i ranging from 1 to 5, are overview STED images of the vimentin filaments. bi) pictures are enlargements of confocal images, corresponding to the location defined by the white squares in the images shown in the panels ai). The ci) images are the STED counterparts to bi), i.e. the enlargements of the areas marked in panels ai). Finally, di) show normalized intensity line profiles of the filaments marked in ci) where the white bars indicate the location of the black and red profiles extracted from the confocal and STED images, respectively. Scales bars represent 1 µm in images. i = 1 corresponds to Oregon-green 488, i = 2 to Chrome 488, i = 3 to Alexa 488, i = 4 to DY495, and i = 5 to FITC.
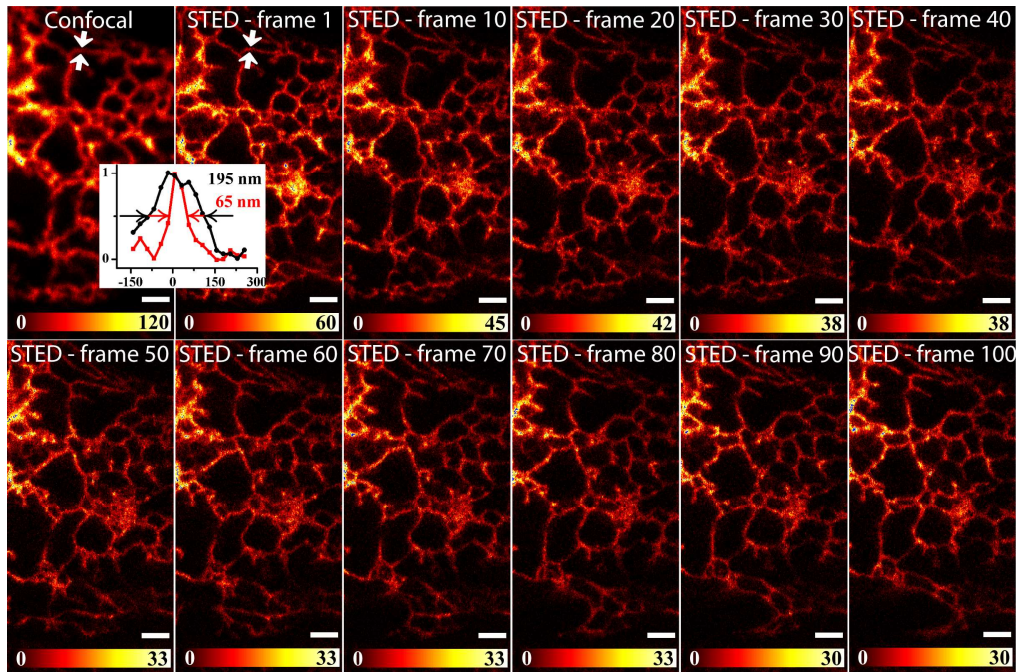
Fig. 4. Intensity-normalized confocal and STED images of the ER of a living PtK2 cell expressing the fluorescent protein Citrine, taken from a time-lapse movie of 100 frames acquired in 190 ms each. The upper left image was recorded in the confocal mode by blocking the STED beam, whereas the other images were recorded in the STED mode. The full movie is available online (Media 1). The fast scanning axis is the vertical axis. Scale bars correspond to 1 µm. Normalized intensity profiles of the images of an ER wall in confocal an STED modes are presented in the inset in black and red, respectively. These profiles correspond to the area located between the arrows in the two upper left frames.

The complete movie is available online, see Fig. 4 (Media 1). Each of the 100 images (12 µm × 6 µm) was acquired in 190 ms, with a dwell-time of 0.94 µs and a pixel size of 25 nm. Although the setup can acquire images successively without any breaks, the chosen time interval between two consecutive frames was 1.5 s in order to see significant displacements of the structures and to allow the exchange of potentially photobleached proteins by fresh ones by diffusion within the ER network. The optical powers used in the back aperture of the objective lens were 35 µW for excitation at 488 nm and ~300 mW for STED at 592 nm. As a reference for comparison, the first image of the series was recorded in the confocal mode by blocking the STED beam.

Sub-diffraction fluorescent structures featuring image intensity profiles having FWHM as small as 65 nm in the STED mode can be found. Since the real size of those structures is unknown, we can only claim that the optical resolution in this case must be < 65 nm. Although the fluorescence signal was slowly decreasing between the first and the last (100th) STED image, the amount of information about the structures was remarkably preserved, at least for following their motions.

4. Discussion and conclusion

While the instrumentation for STED microscopy was perceived to be complex in the past, recent efforts have demonstrated its ease of implementation by simplifying the original experimental design [14,18,19]. The implementation of STED microscopy with CW laser beams is probably the most straightforward version, since it requires no synchronization, pulse length optimization, or timing between the excitation and the STED beams [14]. A drawback of CW fluorescence microscopy is the amount of photo-bleaching when working with fluorescent dyes having a non-negligible triplet build-up [20]. But when combined with a

fast beam-scanner this disadvantage vanishes with the increase in scanning speed since, in the ideal case, the excitation at a given position in the sample occurs in sub-microsecond time windows separated by microseconds [21]. On the other hand the fast beam-scanning configuration benefits from the continuous excitation of fluorophores that provides a higher fluorescence count-rate than with a pulsed excitation, allowing in principle an even faster image acquisition.

While the average power of the STED beam used in the CW mode significantly exceeds (by typically 3-6 fold) the time-averaged power of a typical (80 MHz) pulsed STED system, the focal peak power is lower by about the same factor. Fortunately, the STED beam wavelength is so red-shifted (with respect to the absorption spectrum of the dye) that spurious absorption of the STED beam is minimized. Nonetheless, when operating CW STED microscopy at the highest power levels in living cells, potential detrimental influences have to be considered. In some applications, optical trapping by the STED beam may also play a role. However, this opto-mechanical effect is favorably diverted by the shape of the doughnut and also by the fact that the doughnut area is larger by ~4-fold as compared to a regularly focused beam, which reduces the intensity gradient. In most cases, the doughnut-shape of the STED beam is unfavorable for optical trapping. Besides, the fast scanning employed to suppress photobleaching also suppresses optical tweezing.

So far CW-STED was limited by the availability of high-power sources in the yellow-orange range of the optical spectrum. Owing to the recent development in fiber laser technologies, new sources make the CW-STED implementation a highly appealing approach. Two 1 W lasers were used for this work in order to obtain sufficient power in the back aperture of the objective lens, but a non-negligible part of it was lost in the combination of the two STED beams. Therefore we expect that the use of a single unit of an upcoming higher power version of the same laser will give similar results for less than twice the initial power. Moreover, by using a single STED beam, the remaining intensity in the center of the STED doughnut can only be improved, and the optical alignment can only be easier. The second polarization channel could then be exploited for implementing an axial doughnut in order to also improve the resolution in the third dimension [13]. For excitation, any source providing at least ~300 µW CW light at 488 nm could have been used instead of the Argon ion laser.

In conclusion we have demonstrated that the simple injection of a 592 nm CW laser beam in a fast-scanning microscope, provided by a convenient and economic laser source, allows fast sub-diffraction imaging at a speed of 190 ms per frame with < 65 nm resolution in living cells expressing the fluorescent protein Citrine. An even higher resolution < 60 nm was obtained in fixed samples stained with 5 different commonly used fluorescent markers. The recent emergence of high-power CW solid-sate lasers at other wavelengths, such as 580 nm, 628 nm, 642 nm, and other wavelengths will certainly complete the already rich variety of fluorescent probes suitable for STED microscopy [22], allowing easy-to-implement high-speed multicolor CW-STED imaging.